Bio-Design and Manufacturing (2024) 7:307–319
https://doi.org/10.1007/s42242-024-00271-9

RESEARCH ARTICLE

Oxygen tension modulates cell function in an in vitro three-dimensional glioblastoma tumor model

Sen Wang[1,2,3] · Siqi Yao[1,2,3] · Na Pei[1,2,3] · Luge Bai[1,2,3] · Zhiyan Hao[1,2,3] · Dichen Li[1,2,3] · Jiankang He[1,2,3] · J. Miguel Oliveira[4,5] · Xiaoyan Xue[6] · Ling Wang[1,2,3] · Xinggang Mao[7]

Received: 20 July 2023 / Accepted: 30 January 2024 / Published online: 13 April 2024

Abstract

Hypoxia is a typical feature of the tumor microenvironment, one of the most critical factors affecting cell behavior and tumor progression. However, the lack of tumor models able to precisely emulate natural brain tumor tissue has impeded the study of the effects of hypoxia on the progression and growth of tumor cells. This study reports a three-dimensional (3D) brain tumor model obtained by encapsulating U87MG (U87) cells in a hydrogel containing type I collagen. It also documents the effect of various oxygen concentrations (1%, 7%, and 21%) in the culture environment on U87 cell morphology, proliferation, viability, cell cycle, apoptosis rate, and migration. Finally, it compares two-dimensional (2D) and 3D cultures. For comparison purposes, cells cultured in flat culture dishes were used as the control (2D model). Cells cultured in the 3D model proliferated more slowly but had a higher apoptosis rate and proportion of cells in the resting phase (G0 phase)/gap I phase (G1 phase) than those cultured in the 2D model. Besides, the two models yielded significantly different cell morphologies. Finally, hypoxia (e.g., 1% O_2) affected cell morphology, slowed cell growth, reduced cell viability, and increased the apoptosis rate in the 3D model. These results indicate that the constructed 3D model is effective for investigating the effects of biological and chemical factors on cell morphology and function, and can be more representative of the tumor microenvironment than 2D culture systems. The developed 3D glioblastoma tumor model is equally applicable to other studies in pharmacology and pathology.

Sen Wang and Siqi Yao have contributed equally to this work.

✉ Ling Wang
menlwang@mail.xjtu.edu.cn

✉ Xinggang Mao
xgmao@hotmail.com

1 State Key Laboratory for Manufacturing System Engineering, Xi'an Jiaotong University, Xi'an 710054, China

2 School of Mechanical Engineering, Xi'an Jiaotong University, Xi'an 710054, China

3 NMPA Key Laboratory for Research and Evaluation of Additive Manufacturing Medical Devices, Xi'an Jiaotong University, Xi'an 710054, China

4 3B's Research Group, I3Bs–Research Institute on Biomaterials, Biodegradables and Biomimetics, University of Minho, Headquarters of the European Institute of Excellence on Tissue Engineering and Regenerative Medicine, AvePark, Zona Industrial da Gandra, 4805-017 Barco, Guimarães, Portugal

5 ICVS/3B's-PT Government Associate Laboratory, 4806-909 Braga/Guimarães, Portugal

6 Department of Pharmacology, School of Pharmacy, Fourth Military Medical University, Xi'an 710032, China

7 Department of Neurosurgery, Xijing Hospital, Fourth Military Medical University, Xi'an 710032, China

Graphic abstract

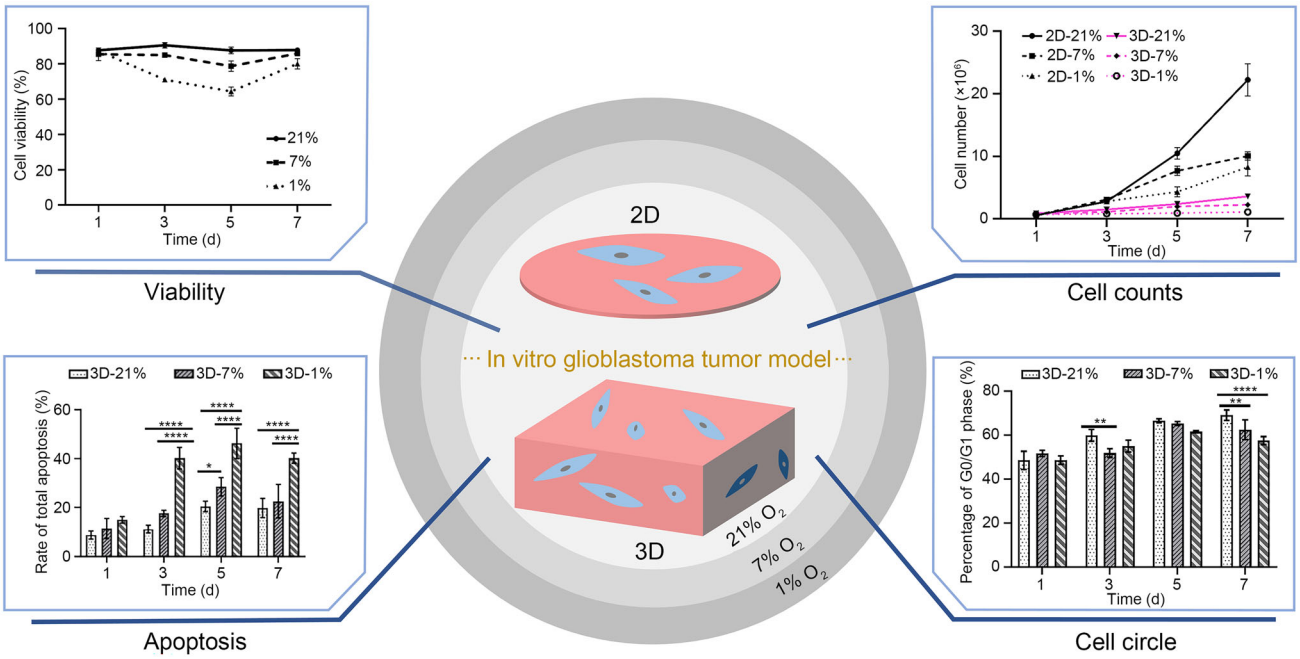

Keywords Hypoxia · Glioma · Three-dimensional glioma model · In vitro

Introduction

Glioblastoma multiforme (GBM) is the most common aggressive malignant tumor [1–3]. Because of the complexity of the tumor microenvironment and the lack of an accurate pathophysiological model, the development of tumor drugs is slow and often fails. Therefore, it is necessary to build a more accurate in vitro tumor model for drug development and tumor pathology research. At present, the main models for drug development of tumor diseases are animal models and two-dimensional (2D) cell culture models. Although the traditional in vitro 2D models are easy to operate and inexpensive, they do not accurately reflect the intricate cell–cell, cell–tissue, and cell–microenvironment relationships. Importantly, 2D models do not retain the heterogeneity of the parent tumor [4]. These issues make it complicated to infer cell migration, cell viability, cell growth, and apoptosis in real tissue using in vitro models [5–9]. As a result, the failure rate of drug development is as high as 95%. Meanwhile, animal models can provide higher tumor microenvironment fidelity [10], but they are usually costly and take time. Besides, differences between species lead to high failure rates in drug development [11].

Therefore, in vitro three-dimensional (3D) tumor models have become widely used in research on antitumor drugs. Such 3D models can better simulate the natural tumor microenvironment, provide the mechanical and biochemical support required for tumor cell growth, and provide a more accurate representation of drug efficacy [12–14]. Florczyk et al. [6] found that GBM cells cultured on a porous chitosan-hyaluronic acid scaffold expressed higher levels of stem cells and cell invasion markers and were more resistant to chemotherapy than when cultured in a 2D model. Using 3D-Alvetex scaffolds, Gomez-Roman et al. [15] showed that extracellular matrix concentrations affected cell growth and cell resistance more than the 3D structure itself did, and that cells cultured under hypoxia (0.5% O_2) exhibited higher drug resistance. However, the materials that they used to construct the 3D model were not optimal for imitating the biochemical components that surround the glioma tissue. The most recognized extracellular matrix change that occurs in tumor tissues is collagen deposition. Glioma tissue contains large amounts of fibrillar collagen [16, 17] which activates the signal transduction network that gliomas need [18]. Collagen promotes the adhesion, movement, proliferation, differentiation, and metastasis of tumor cells [17, 19]. Therefore, selecting appropriate biomaterials (such as collagen) is paramount to construct 3D models accurately simulating the growth of real tumors in vitro.

Increasing evidence indicates that the tumor microenvironment is pivotal for the fate of GBM cells and tumor progression [5, 20]. It is a complex and dynamic system

[21], and hypoxia is one of its key aspects. As glioblastomas grow fast, the supply of blood vessels to the tumor becomes insufficient [3], which can limit oxygen diffusion within the tumor tissue. In the body, the oxygen tension in glioblastomas ranges from 0.1% to 10% [3, 22]. This value is much lower than the 21% O_2 level that is used for in vitro tumor cell culture. Hypoxia can increase the expression of the tumor stem cell marker CD133 [3, 23]. Hypoxia can also increase the resistance of tumor cells to chemical drugs and radiation [24, 25]. Liverani et al. [26] demonstrated that hypoxia can affect the growth kinetics of cells and endow cells in 3D collagen-based scaffolds with invasive characteristics. Current research on hypoxia in 3D models cultured 3D tissues under 21% O_2 to investigate the effects of hypoxia caused by the 3D model itself on the growth of glioma cells. However, few studies have investigated the effect of hypoxic conditions on the growth of glioma cells by culturing 3D tissues under 1% or 7% O_2. Therefore, culturing 3D tissues under a hypoxic atmosphere of 1% or 7% O_2 is of great significance for better understanding the effects of hypoxia on tumor cell growth and screening suitable anticancer drugs.

In this study, we constructed a 3D tumor model of human primary glioblastoma using a collagen-based hydrogel and cultured it in vitro under various oxygen concentrations to document the effects of oxygen concentration on the tissue. Next, we explored the differences in cell proliferation, morphology, apoptosis rate, and cell cycle of U87MG (U87) cells cultured in 2D and 3D models. Moreover, we investigated the effects of oxygen concentration on the tissue and cell viability of U87 cells cultured in 3D collagen blocks.

Materials and methods

Preparation of the 3D tumor model

We prepared the cell-laden hydrogel as described previously [27–29]. We mixed a rat tail-derived type I collagen solution (4 mg/mL in 0.1 mol/L glacial acetic acid) with complete Dulbecco's modified eagle medium (DMEM, HyClone, USA) at a volume ratio of 1:1. We adjusted the pH of the mixed collagen and medium solution to 7.4 using 0.5 mol/L NaOH (Tianli, China). Then, we mixed the collagen–medium mixture with U87 cell precipitation at 4 °C to obtain a cell–collagen mixture with a cell concentration of 1×10^6 cells/mL. Next, we injected the mixed cell–collagen solution into a mold made of polydimethylsiloxane (PDMS, Dow Corning, USA) and cultured it in a cell culture incubator at 37 °C for 40 min. Finally, we obtained 3D collagen samples of 10 mm × 10 mm × 2 mm by demolding them from the mold.

2D and 3D cell culture

We purchased human glioblastoma U87 cells from Shanghai Genechem Co., Ltd. (China) and cultured them in DMEM supplemented with 10% newborn calf serum (GIBCO BRL, Invitrogen, USA). U87 cell lines were authenticated with short tandem repeats in 2018. The institutional review board of the Xijing Hospital of the Fourth Military Medical University approved the study protocol. For 2D culture, we cultured U87 cells in a monolayer cell culture dish at a density of 1×10^4 cells/cm^2 and supplemented them with complete DMEM containing 10% fetal bovine serum (FBS, Gibco, USA) and 1% penicillin/streptomycin (HyClone, USA). We replaced the medium every two days. For 3D culture, we cultured the prepared 3D tumor models in the same culture medium. We cultured all cells in incubators at different oxygen concentrations (21%, 7%, or 1%) and evaluated them on Days 1, 3, 5, and 7.

We achieved the different oxygen concentrations by culturing cells in three triple-gas incubators (PH-1-A, Wuxi Puhe Biomedical Technology, China) with different sets of oxygen concentrations. We maintained the cells at 21%, 7%, and 1% O_2 in parallel for seven days and seeded all the cells at Passage 15.

Cell morphology

We collected cells on Days 1, 3, 5, and 7 for morphology examination. For the 2D samples, we observed and photographed the morphology of U87 cells under an inverted fluorescence microscope (Ti-S, CHANSN, China). For the 3D samples, we fixed the 3D collagen samples with 4% paraformaldehyde for 1 h, and then cut them into 80-μm-thick slices with a freezing microtome and observed and photographed the morphology of U87 cells in 3D culture under a laser scanning confocal microscope (LSCM, A1, Nikon, Japan) in a bright field.

Cell proliferation

We digested the 2D-cultured U87 cells with a trypsin solution (HyClone, USA) for 2 min and terminated the digestion with cell culture medium. We then collected the cells and centrifuged them at 1000 r/min in a centrifuge (HC-3018r, Zonkia, China) for 3 min. After discarding the supernatant, we added 3 mL of cell culture medium to the evenly mixed cells. Then, we injected 20 μL of this cell suspension into a cell counting plate (SD1300, Nexcelom, USA) and counted the cells using a cell counting instrument (Nexcelom, USA). We digested the 3D samples with type I collagenase (DIY-

IBio, China) for 80 min under the corresponding culture conditions. Finally, we centrifuged the cells at 1000 r/min for 3 min. The subsequent processing method was the same as for the 2D samples.

Cell viability

We collected the 2D or 3D samples cultured under different oxygen concentrations (21%, 7%, and 1%) at various time points (on Days 1, 3, 5, and 7) and determined the viability of cells using a LIVE/DEAD® Viability/Cytotoxicity Kit (L3224, Thermo, USA). This kit stains the living cells with green fluorescence and the dead cells with red fluorescence. Cell viability was expressed as the proportion of green cells over the total number of stained cells. We recorded stained cell images using an LSCM. We analyzed at least three samples at each time point.

Immunofluorescence staining

We collected 2D and 3D samples at different time points (on Days 1, 3, 5, and 7), fixed them in 4% paraformaldehyde (Solarbio, China) for 1 h, and washed them three times with 1× phosphate-buffered saline (PBS, HyClone, USA) for 5 min each time. Then, we sliced the 3D samples with a freezing microtome (LEICA, Germany) for immunofluorescence staining. Each slice was 80 μm thick. Then, we blocked all 2D and 3D samples with 5% goat serum (Boster, USA) for 1 h at 37 °C and incubated them overnight at 4 °C with primary antibodies (Table 1) and 0.3% Triton X-100 (Solarbio, China). We then washed the samples six times with 1× PBS for 10 min each time. After that, we incubated the samples with secondary antibodies for 4 h at room temperature. Subsequently, we added 4,6-diamino-2-phenyl indole (DAPI, Invitrogen, USA). After 15 min, we washed the samples six times with 1× PBS and observed them under the LSCM. Table 1 lists the types and proportions of antibodies used.

Table 1 Summary of antibodies used in this study

Antibody type	Antibody name	Proportion in 2D models	Proportion in 3D models
Primary antibody	Ki-67 (8D5) mouse mAb (9449s, CST, USA)	1:800	1:800
	Rabbit anti-GFAP (ab7260, Abcam, USA)	1:1000	1:500
Secondary antibody	Donkey anti-rabbit (A-21206, Invitrogen, USA)	1:1000	1:500
	Donkey anti-mouse (A-31570, Invitrogen, USA)	1:1000	1:400

GFAP: glial fibrillary acidic protein

Flow cytometry: detection of cell cycle and apoptosis rate

After digestion, we collected cells from the 2D and 3D models for flow cytometry (see Sect. "Cell morphology" for details). To determine the cell cycle, we fixed the samples with 70% ethanol at 4 °C for 4 h and then washed them with 1× PBS three times. We then resuspended the cells in 400 μL of 1× PBS containing 50 μL of propidium iodide (PI) and 50 μL of RNase (Boster, USA) and incubated them in the dark for 1 h at room temperature. We then processed the samples using a flow cytometer (Coulter-XL, USA).

To detect apoptosis, we washed the samples with 1× PBS three times. Then, we resuspended the cells with 100 μL of binding buffer containing 5 μL of Annexin V-FITC and 10 μL of PI (Boster, USA) and incubated them in the dark for 1 h at 4 °C. Finally, we added binding buffer to reach a total volume of 500 μL and tested the samples.

Statistical analysis

We analyzed all the data in GraphPad Prism8 (GraphPad, USA). We performed at least three independent replicates for each experiment. Data are expressed as mean±standard deviation (SD), with n indicating the number of replicates. We compared the groups using two-way analysis of variance (ANOVA) (e.g., $^{*}P<0.05$, $^{**}P<0.01$, $^{***}P<0.001$, $^{****}P<0.0001$).

Results

Comparison of cell morphology and cell counts in the 2D and 3D models

After being cultured under 21% O_2 for three days, the U87 cells from the 2D culture (Fig. 1a) exhibited long spindle shapes, while those cultured in 3D collagen blocks exhibited a large diversity in cell morphology (Fig. 1b), showing both long spindle and spherical shapes.

To assess the effect of 2D and 3D culture conditions on the growth rate of U87 cells, we counted cells on Days 1,

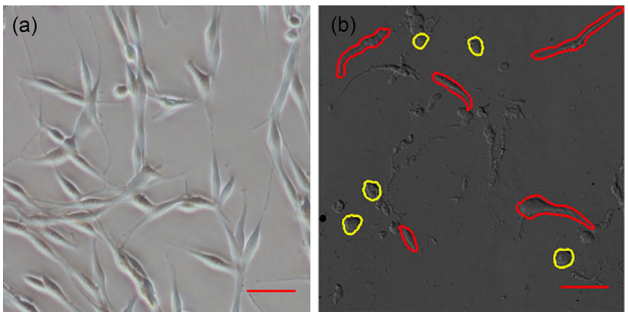

Fig. 1 Morphology comparison of U87 cells cultured in 2D or 3D models for three days under 21% O_2. **a** Morphology of cells from 2D culture (inverted fluorescence microscope). **b** Morphology of cells from 3D collagen blocks (LSCM). Red outlines indicate spindle shapes and yellow outlines indicate spherical shapes. Scale bar: 50 μm. U87: U87MG; 2D: two-dimensional; 3D: three-dimensional; LSCM: laser scanning confocal microscope

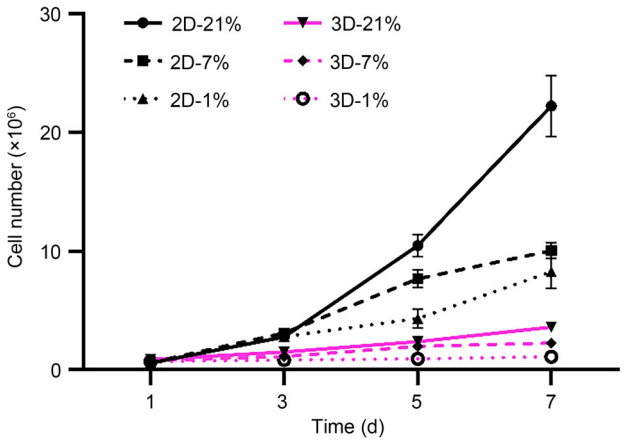

Fig. 2 Cell counting results for 2D or 3D cultures with 1%, 7%, and 21% O_2 in the culture environment. Data are expressed as mean±SD ($n \geq 3$). 2D: two-dimensional; 3D: three-dimensional; SD: standard deviation

3, 5, and 7. U87 cells in 3D collagen blocks grew more slowly than those cultured in 2D models at the tested oxygen concentrations (Fig. 2). Under 21% O_2, the number of U87 cells in 2D culture increased exponentially from $(0.579\pm0.023)\times10^6$ cells on Day 1 to $(22.235\pm2.586)\times10^6$ cells on Day 7, while that of cells in 3D collagen blocks slowly increased from $(0.878\pm0.080)\times10^6$ cells on Day 1 to $(3.609\pm0.282)\times10^6$ cells on Day 7. Additionally, under both 2D and 3D culture conditions, the number of U87 cells increased with increasing oxygen concentrations.

Comparison of cell cycle state and apoptosis rate of cells in 2D and 3D cultures

To assess the effects of 2D or 3D culture conditions on the cell cycle of U87 cells, we carried out flow cytometry analyses on Days 1, 3, 5, and 7. As shown in Fig. 3, in 3D collagen blocks, more U87 cells were in the resting phase (G0 phase)/gap I phase (G1 phase) and fewer were in the DNA synthesis phase (S phase) than in 2D culture. In addition, regardless of culture conditions, the G0/G1 population progressively increased while the S population decreased. This result was consistent with the slower proliferation of cells in 3D collagen blocks than in 2D culture (Fig. 2). Consistently, there was no significant difference in the proportion of cells in the G II (G2)/mitotic (M) phase in 2D or 3D cultures (Fig. 3b).

To investigate whether culture conditions altered the viability and apoptosis rate of U87 cells, we carried out flow cytometry at various time points (Days 1, 3, 5, and 7). The survival rate of U87 cells in 3D collagen blocks was slightly lower than that in 2D culture, and was constantly at above 85% (Fig. 4a). This result suggests that the 3D collagen blocks constructed in this study have good cytocompatibility and are suitable for the growth of U87 cells. As shown in Figs. 4b–4d, the late apoptosis rate of U87 cells in 3D collagen blocks remained 5%–10%, higher than that of cells in 2D culture (below 5%). The early apoptosis rate of U87 cells in 3D collagen blocks increased from (3.2±0.2)% on Day 1 to (12.7±3.3)% on Day 7, while that of cells in 2D culture remained below 5%. Besides, the total apoptosis rate of U87 cells indicated the similar tendency as mentioned above within seven culturing days.

Effect of oxygen concentration on the viability of cells cultured in 3D collagen blocks

We determined the viability of U87 cells cultured in 3D collagen blocks under various oxygen concentrations by live/dead assay and flow cytometry at different time points (Days 1, 3, 5, and 7). As shown in Fig. 5a, most cells remained alive (green), and only few dead cells (red) were observed. In addition, U87 cell viability decreased with decreasing oxygen concentration in the culture environment, and the cells in 1% O_2 had the lowest survival rate (Fig. 5b). On Day 7, the survival rates for cells under 21%, 7%, and 1% O_2 were (87.80±1.23)%, (85.87±0.59)%, and (80.07±2.94)%, respectively. Moreover, the survival rate for cells under 21% O_2 was nearly constant over time, whereas that for cells under 1% and 7% O_2 decreased in the first five days of culture and increased on Day 7, and the changes in the cells under 1% O_2 were more dramatic than those under 7% O_2.

Effect of oxygen concentration on the apoptosis rate of cells cultured in 3D collagen blocks

To document the effects of oxygen concentration on the apoptosis of U87 cells in 3D collagen blocks, we cultured the 3D samples under various oxygen concentrations and determined the apoptosis rates by flow cytometry at different time points (Days 1, 3, 5, and 7) (Fig. 6a). The early apoptosis

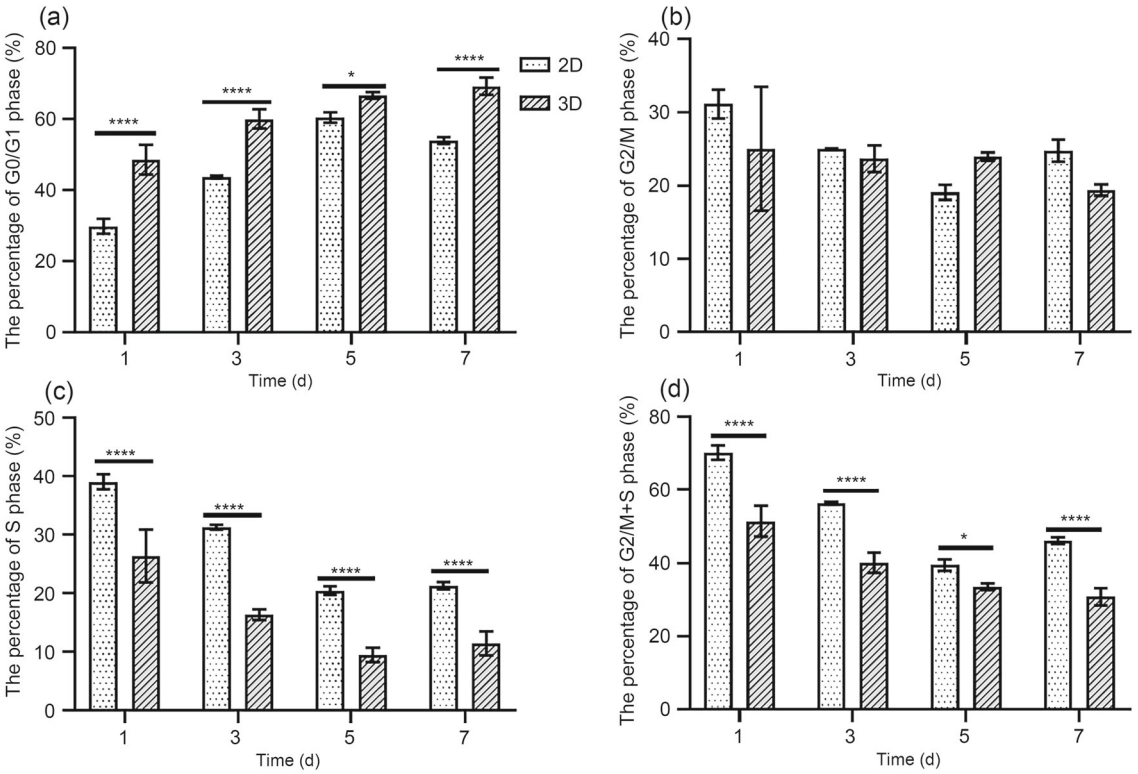

Fig. 3 The effect of 2D or 3D culture conditions on cell cycle at various time points, as determined by flow cytometry: **a** G0/G1 phase; **b** G2/M phase; **c** S phase; **d** G2/M+S phase. Data are expressed as mean±SD ($n \geq 3$) and were analyzed by two-way ANOVA. $^{*}P<0.05$, $^{****}P<0.0001$. 2D: two-dimensional; 3D: three-dimensional; SD: standard deviation; ANOVA: analysis of variance

rate of U87 cells in 3D collagen blocks increased over time (Fig. 6b) regardless of the oxygen concentration. Moreover, lower oxygen concentrations in the culture environment led to higher proportions of cells in early apoptosis. Relative proportion of early apoptosis of U87 cells under 21% O_2 increased from (3.20±0.30)% on Day 1 to (12.70±3.30)% on Day 7, and that of cells under 1% O_2 increased from (7.70±1.39)% on Day 1 to (29.60±3.29)% on Day 7.

Meanwhile, lower oxygen concentrations in the culture environment increased late apoptosis rates. Cells under 21% O_2 had the lowest late apoptosis rate while those under 1% O_2 had the highest. Furthermore, the late apoptosis rate of U87 cells under 21% O_2 barely increased over time—going from (5.57±1.35)% on Day 1 to (7.13±1.05)% on Day 7 (Fig. 6c). Conversely, the late apoptosis rate of U87 cells under 1% O_2 increased from (7.27±0.12)% on Day 1 to (21.90±2.98)% on Day 5 and then decreased to (10.57±1.32)% on Day 7. The same tendency was observed in cells under 7% O_2, but with a smaller fluctuation range. The total apoptosis rates also indicated the similar tendency (Fig. 6d). These results indicate that hypoxic (e.g., 1% or 7% O_2) conditions may promote apoptosis in 3D culture.

Effects of oxygen concentration on cell cycle and proliferation of cells cultured in 3D collagen blocks

To assess the effects of oxygen concentration on the proliferation of U87 cells cultured in 3D collagen blocks, we determined the cell cycle states at various time points (Days 1, 3, 5, and 7) using flow cytometry. As shown in Figs. 7a and 7b, from Day 1 to Day 5, the proportion of cells in the G0/G1 phase increased in all oxygen concentration sets. From Day 5 to Day 7, the 21% O_2 group continued to rise, while the 1% and 7% O_2 groups turned to decrease. As for the proportion of cells in the G2/M phase, all the groups showed decreasing tendency within seven culturing days. Moreover, from Day 3 to Day 7, samples cultured under 21% O_2 had a higher proportion of cells in the G0/G1 and G2/M phases than those cultured under 7% or 1% O_2. Additionally, the difference of the proportion of cells in the S phase between 1% and 21% O_2 (Fig. 7c) significantly increased over time, with 3.17% on Day 1, 12.47% on Day 3, 13.44% on Day 5, and 19.58% on Day 7. Finally, the proportion of cells in the G2/M + S phase decreased over time in cells cultured under 21% O_2. However, in cells cultured under 1% and 7% O_2, it decreased during the first five days and then increased on the seventh day (Fig. 7d).

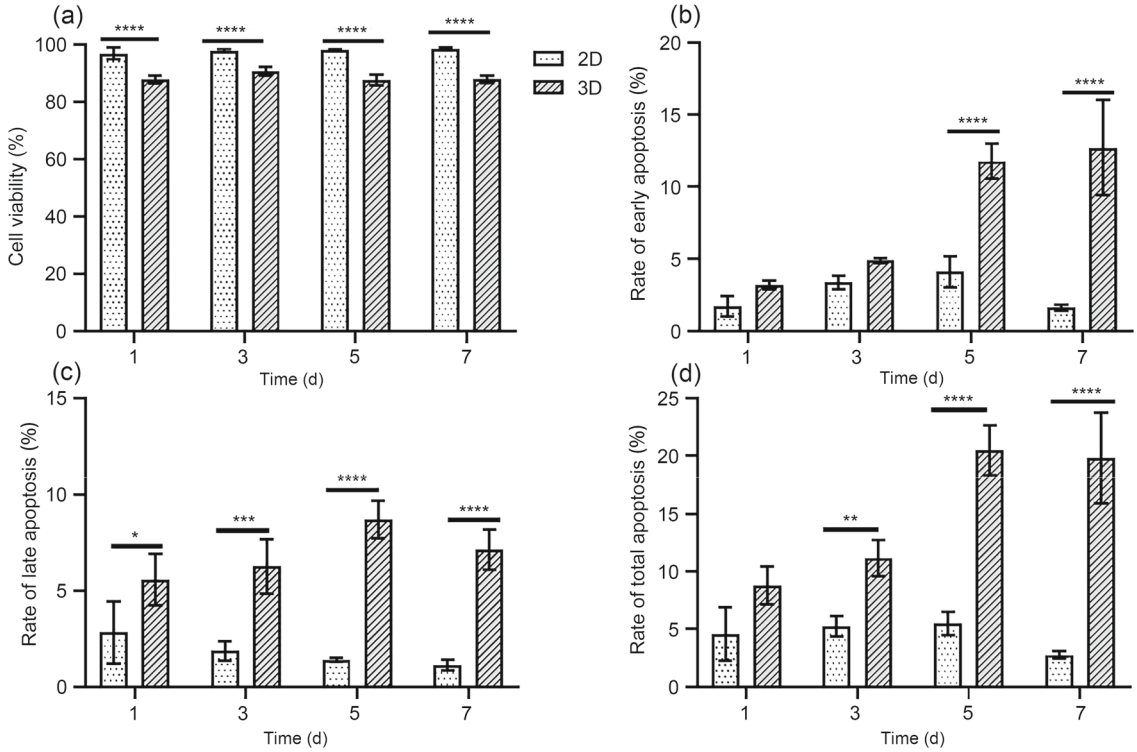

Fig. 4 The effects of 2D or 3D culture conditions on the viability and apoptosis rate of U87 cells at various time points, as determined by flow cytometry: **a** cell viability; **b** early apoptosis rates; **c** late apoptosis rates; **d** total apoptosis rates. Data are expressed as mean±SD ($n \geq 3$) and were analyzed by two-way ANOVA. $^{*}P<0.05$, $^{**}P<0.01$, $^{***}P<0.001$, $^{****}P<0.0001$. 2D: two-dimensional; 3D: three-dimensional; U87: U87MG; SD: standard deviation; ANOVA: analysis of variance

To assess the proliferation potential, we stained the nuclei of proliferating cells with Ki-67. The images indicated that the cells cultured under all three oxygen concentrations had a good potential for proliferation (Fig. 8).

To verify the correlation between cell morphology in the 3D collagen blocks and oxygen concentration in the culture environment, we cultured the 3D samples under different oxygen concentrations and stained the U87 cells with glial fibrillary acidic protein (GFAP). Figure 8 shows typical fluorescence images of the 3D samples cultured under different oxygen concentrations. The images indicate that under 1% O_2, most U87 cells showed spherical shapes (independently of culture duration) and a few cells at the edges of the 3D collagen blocks showed spindle shapes (Fig. S1 in Supplementary Information). Under 21% O_2, some cells changed from spherical to spindle shapes over time and some remained spherical (Fig. 8). The images indicate that the number of cells in 1% O_2 changed more slowly than that in 21% or 7% O_2, which is consistent with the results shown in Fig. 2.

Discussion

Two-dimensional cell culture models may only marginally resemble the microenvironment of natural tissue, resulting in significant discrepancies between results obtained from 2D cell culture models and those from natural tissues in pathological research and antitumor drug development [10, 11]. In this study, we constructed an in vitro 3D tumor model based on type I collagen to quantitatively study the contributions of 2D and 3D culture environments to the morphology and functional development of U87 cells. Moreover, hypoxia is a typical feature of gliomas and is related to poor prognoses [24]. Therefore, we thoroughly investigated the effects of culturing environments with various oxygen concentrations on the growth of U87 cells embedded in 3D models, and discussed the synergistic effects of the culturing configuration and hypoxia.

The dimensionality of culturing models could significantly affect the morphology of U87 cells. We found that U87 cells cultured under 21% O_2 in 3D collagen blocks

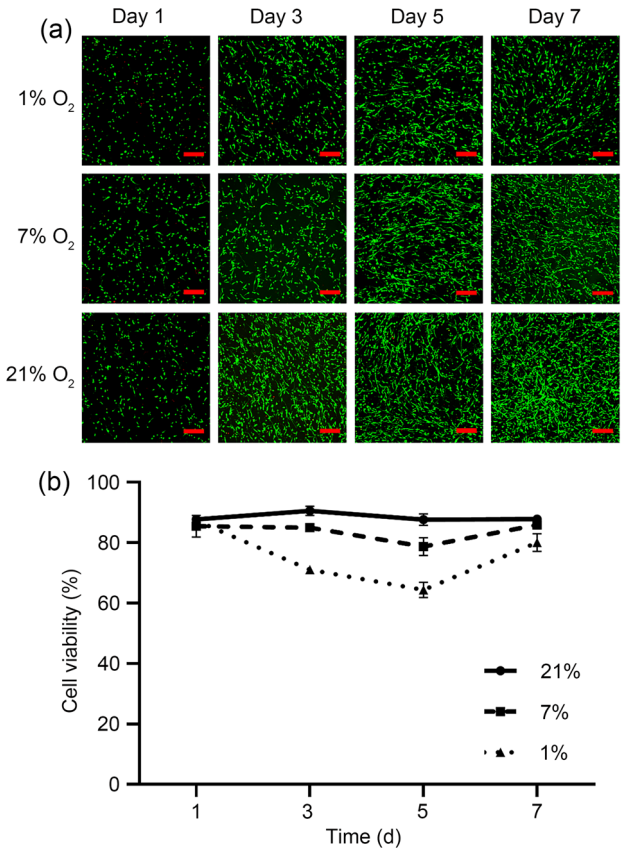

Fig. 5 Effect of oxygen concentration on the survival rate of U87 cells cultured in 3D collagen blocks. **a** Fluorescence images of 3D samples cultured under different oxygen concentrations at different time points (Days 1, 3, 5, and 7). The living cells were stained with a green fluorescent marker and dead cells were stained with a red fluorescent marker. Scale bar: 200 μm. **b** The survival rates of the cells cultured in 3D collagen blocks under different oxygen concentrations were determined by flow cytometry, and the data are expressed as mean±SD ($n \geq 3$). U87: U87MG; 3D: three-dimensional; SD: standard deviation

showed morphology diversity, with spherical and spindle-shaped cells, while those in the 2D culture all exhibited long spindle shapes. Consistent with previous research, primary tumor cells cultured in 3D collagen scaffolds were morphologically similar to glioma cells in human tumor tissues; i.e., they all exhibited spherical shapes [16]. Liverani et al. [26] also indicated that the cells of human breast cancer cell line (MDA-MB-231) and human breast adenocarcinoma cell line (MCF-7) encapsulated within 3D scaffolds displayed morphological similarities to matching xenograft tumor cells. The morphology difference of the cells in the 2D or 3D models indicated that dimensionality is an important factor to consider when constructing in vitro tumor models [5]. In vivo, cells need to overcome the physical constraints of the surrounding extracellular matrix to grow and migrate, while these constraints are absent in 2D culture settings. Compared with 2D culture, the 3D culture environment can emulate these physical constraints, which profoundly affect cellular morphology.

We also compared the proliferation rates of U87 cells in 3D collagen blocks and 2D culture over seven days of in vitro culture. We found that the U87 cells in 2D culture showed a typical proliferation curve with an exponential trend, while those in 3D collagen blocks grew more slowly. Moreover, the 3D matrix led to a graduated distribution of oxygen, nutrients, and growth factors; therefore, the cells in 3D collagen blocks had different proliferation rates. Although cells in 2D culture had a relatively uniform proliferation rate, they grew faster than those in 3D collagen blocks [11]. Liverani et al. [26] found that, although cell counts in 3D models increased more slowly than those in 2D culture, the multiple changes in cell numbers in 3D models matched the multiple changes in xenograft tumor volumes. These results indicated that a 3D culture can precisely mimic the growth rate of natural tumors in vitro. Dai et al. [30] showed that in the first 13 days of culture, cells in 2D models had a higher growth rate than those cultured in a 3D environment; however, after 13 days of culture, the cells in the 3D culture grew faster. These results indicated that the 3D model provided an ideal tool for long-term in vitro cell culture.

The oxygen concentration in the culture environment can also significantly impact the proliferation rate of cells. Regardless of culture setting (2D or 3D), decreasing oxygen concentration slowed cell growth. Previous research has also indicated that in 2D culture, cells under 1% O_2 grew slower than cells under 21% O_2 [3, 31]. However, the study of Richards et al. [32] showed that pathophysiological levels of hypoxia (1% O_2) barely affected the proliferation and viability of GBM cells in 2D culture. These differing research results may be related to inconsistencies in the detection methods or cell types. Musah-Eroje and Watson [3] demonstrated that glioma cells in 2D culture could adapt to a hypoxic microenvironment (1% O_2) by reducing their proliferation and enhancing metabolism. This research demonstrated that the mechanisms of cell metabolism changed as the oxygen concentration changed [26, 33]. Therefore, the cell proliferation rates determined via the cell counting kit-8 (CCK-8) or methyl thiazolyl tetrazolium (MTT) kits may not be sufficiently accurate, especially for the 3D models.

In this study, we determined the proliferation rate of U87 cells by cell counting, which precisely reflected changes in cell numbers and the proliferation potential. Slow cell proliferation may be related to the stagnation of the cell cycle or an increase in apoptosis [32]. Additionally, we found that, in the 3D collagen blocks, the proportion of cells in the G0/G1 phase did not depend on oxygen concentration. Meanwhile, decreasing oxygen concentration increased the apoptosis rate—the total apoptosis rate of cells under 1% O_2 reached (40.17±2.10)%. These results suggest that, as the

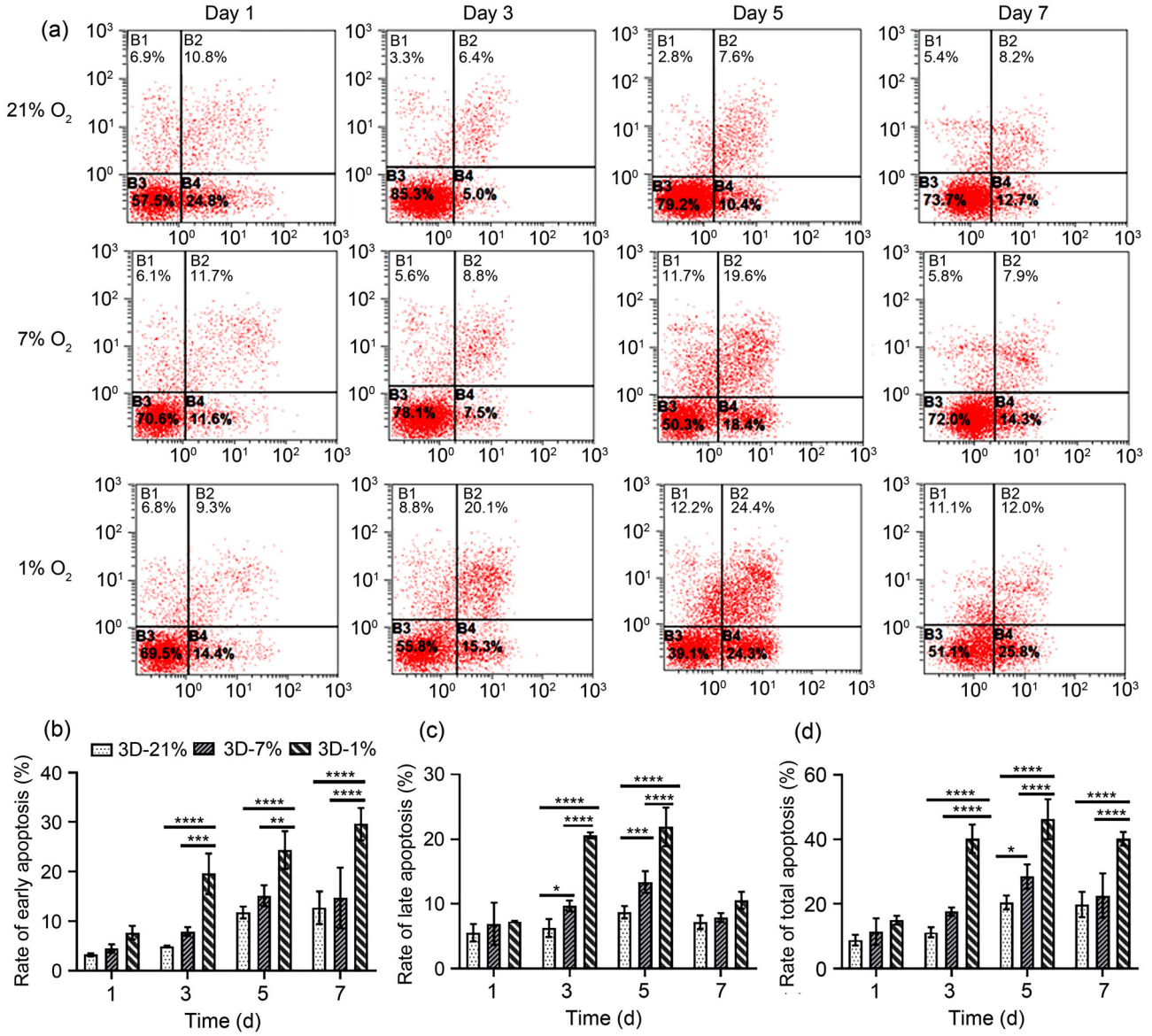

Fig. 6 Effects of different oxygen concentrations (1%, 7%, and 21%) on the apoptosis rates of U87 cells cultured in 3D collagen blocks: **a** representative images of PI-Annexin V staining by flow cytometry; **b** early apoptosis rates; **c** late apoptosis rates; **d** total apoptosis rates. Data are expressed as mean±SD ($n \geq 3$) and were analyzed by two-way ANOVA. $^{*}P<0.05$, $^{**}P<0.01$, $^{***}P<0.001$, $^{****}P<0.0001$. U87: U87MG; 3D: three-dimensional; PI: propidium iodide; SD: standard deviation; ANOVA: analysis of variance

oxygen concentration in the culture environment decreased, the lower proliferation rate of U87 cells in 3D collagen blocks may have been caused by increased apoptosis. In addition, the 3D matrix can constrain the growth rate of U87 cells.

At the same time, the increased proportion of cells in the quiescent stage was related to the enhancement of cell stemness and drug resistance of tumor cells [6, 15]. The drug resistance of stem cells was higher than that reported for glioma cells [30]. The 3D culture environment can increase drug resistance, which can be attributed to the repair of DNA damage and increase in cell stemness [16]. The hypoxic environment can also enhance the stemness and drug resistance of tumors [11, 15, 31, 34, 35]. The enhanced stemness phenotype is associated with an increased proportion of cells in the G0/G1 phase and cellular dedifferentiation [16]. These results are consistent with our findings, showing that the proportion of cells in the G0/G1 phase in 3D culture was higher than that in 2D culture. These results indicated that the 3D collagen glioma models constructed in this study showed enormous potential for studying the mechanisms of tumor

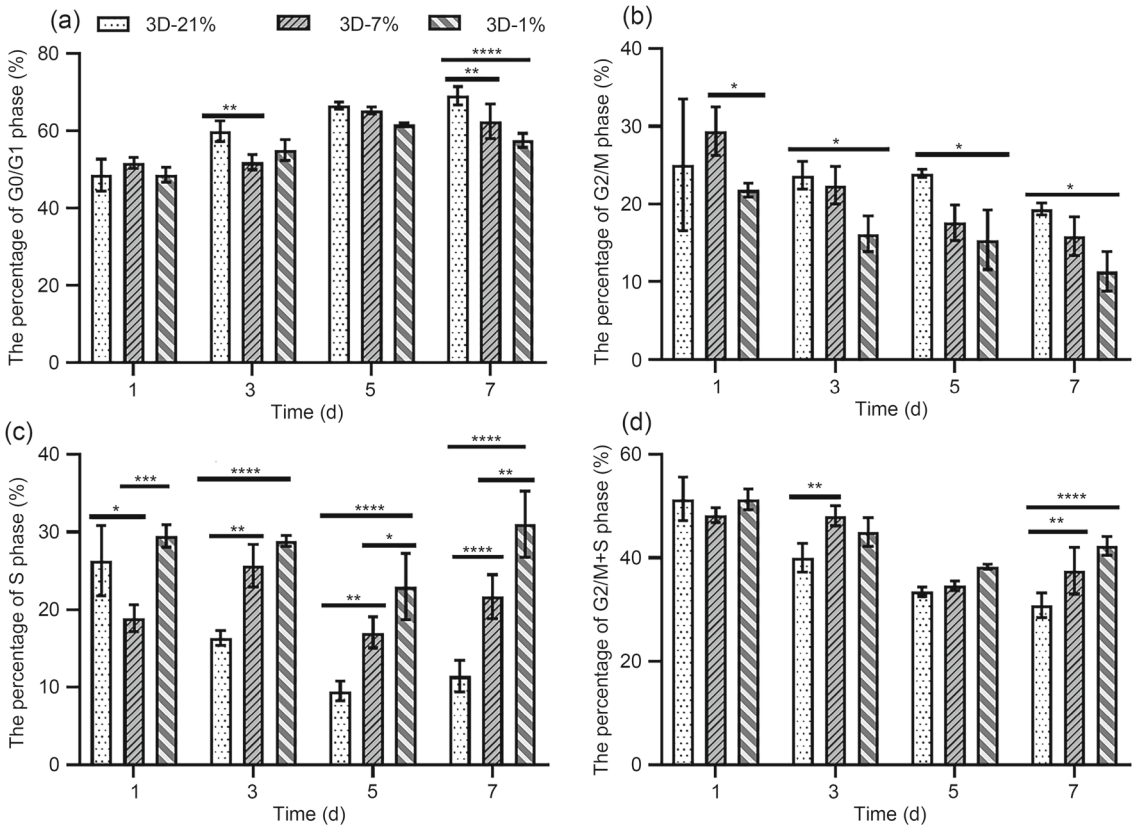

Fig. 7 Effects of oxygen concentration on the cell cycle of U87 cells in 3D collagen blocks: percentage of cells in the G0/G1 phase (**a**), G2/M phase (**b**), S phase (**c**), and G2/M+S phase (**d**) with different oxygen concentrations during seven culturing days. Data are expressed as mean±SD ($n \geq 3$) and were analyzed by two-way ANOVA. $^{*}P<0.05$, $^{**}P<0.01$, $^{***}P<0.001$, $^{****}P<0.0001$. U87: U87MG; 3D: three-dimensional; SD: standard deviation; ANOVA: analysis of variance

resistance as well as relevant targeted therapies. Other studies have also shown that stem cells grow more slowly than their differentiated progeny cells [36, 37], which can also correspond to the changes in cell proliferation rates mentioned above. In other words, the number of cells in 3D collagen blocks changed more slowly than that in 2D culture. As the oxygen concentration decreased, the number of cells also decreased, regardless of the culture dimension. However, our results showed that when cells were cultured in 3D collagen blocks, changing the oxygen concentration in the culture environment did not significantly affect the proportion of cells in the G0/G1 phase, and the reason for this remains to be further studied.

The apoptosis rates of the U87 cells in 3D collagen blocks increased significantly as the oxygen concentration decreased. Due to the limitations of the 3D matrix [15], even for samples cultured in 20% O_2, the oxygen concentration in the 3D-Alvetex scaffold ranged from 2.6% to 8.48%, much lower than that in a 2D culture environment. Therefore, for cells cultured in 3D collagen blocks under 1% O_2, the actual

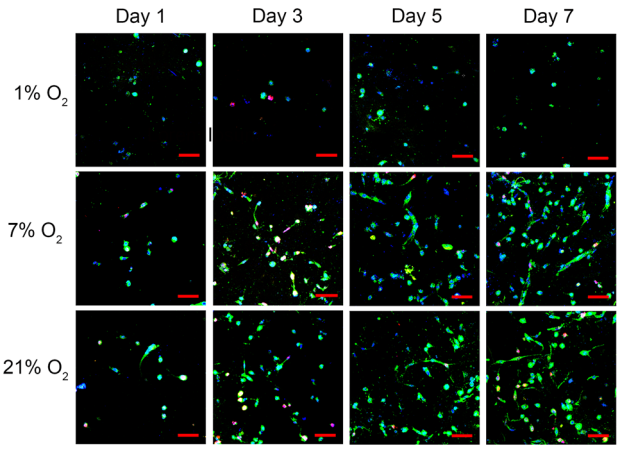

Fig. 8 Representative immunofluorescence images of the 3D samples cultured under different oxygen concentrations on Days 1, 3, 5, and 7. The U87 cells were stained with GFAP and appear in green. The nuclei were counterstained with DAPI and appear in blue. The nuclei of proliferating cells were stained with Ki-67 and appear in red. Scale bar: 50 μm. 3D: three-dimensional; U87: U87MG; GFAP: glial fibrillary acidic protein; DAPI: 4,6-diamino-2-phenyl indole

oxygen tension surrounding the cells was even lower, possibly increasing the apoptosis rate.

Notably, over the seven-day culture timeline, the fifth day seemed to be a turning point. Indeed, on Day 5, the cell survival rate switched from a continuous decline to an increase, and the late apoptosis rate switched from a continuous increase to a decrease, while the proportion of cells in the G2/M+S phase showed an opposite trend to the late apoptosis rate. It can be inferred that the turn of cell survival rate on the fifth day is correlated with the late apoptosis rate and proliferation ratio. This fluctuation became more dramatic as the degree of hypoxia increased.

One of the main reasons for the incurability of GBM is that GBM cells infiltrate adjacent tissues, causing incomplete resection and recurrence [10, 38]. Recent studies have shown that the markers related to cell invasion (e.g., matrix metalloproteinases-2 (MMP-2) and MMP-9) were mostly upregulated in the 3D scaffold [39]. The expression levels of MMP were 2–5 times higher in cells cultivated in 3D scaffolds than those in 2D models [6]. In addition, hypoxia may promote the migration of glioma cells [31, 40]. Many cells cultured in 3D blocks for seven days under 21% O_2 migrated to the edge of the blocks, while cells under 1% O_2 were uniformly distributed in the 3D blocks (Fig. S2 in Supplementary Information). This may indicate that an appropriate oxygen gradient can promote the migration of glioma cells and mimic the in vivo invasive process, as cells migrate to favorable niches to enhance their viability [26]. Meanwhile, severe hypoxia may hinder cell migration.

The tumor microenvironment has various properties [10], including cell–cell interactions [9], gradient distributions of biochemical factors [11], extracellular matrix components [41], complex tissue structures [10, 42, 43], high vascularization levels [32], and matrix stiffness [44]. The oxygen level is only one of these properties and, although the 3D model built in this study cannot perfectly replicate the tumor microenvironment, the oxygen tension could be used for a parametric study on the influence of oxygen concentration on the status of cells in 3D cultures. However, our research also has some limitations. The main component of the constructed 3D model was type I collagen, but the natural extracellular matrix around GBM is composed of various types of extracellular matrix proteins (such as hyaluronic acid) and glycosaminoglycan [45, 46]. Additionally, more and more studies have shown that astrocytes, macrophages, microglia, tumor-associated fibroblasts, and other cells [41, 46–49] may profoundly affect tumor formation in vivo. Therefore, in future studies, 3D matrix that encapsulates the cells should be further optimized, and co-culturing tumor cells with other cells needs to be considered to better mimic the microenvironment of natural tumor tissue.

Conclusions

In this study, we used type I collagen to construct a 3D glioma tumor model and investigated the growth of glioma cells in this setting. We found that U87 cells in the 3D collagen blocks had a high survival rate. Besides, compared to the 2D culture, the morphology of cells cultured in 3D collagen blocks was more similar to that of cells in real tissues, indicating that the proposed 3D glioma tumor model more accurately simulated the growth of glioma cells in vivo. Next, we used the 3D glioma models to explore the effect of oxygen concentration on glioma cell growth in the 3D models. Regardless of the culture setting (2D or 3D), decreasing oxygen concentration slowed the cell proliferation. In 3D collagen blocks, severe hypoxia (1% O_2) significantly increased the apoptosis rate, but general hypoxia (7% O_2) barely affected apoptosis compared with 21% O_2. In addition, the proportion of cells in the G0/G1 phase in 3D culture was higher than that in 2D culture. Furthermore, in 3D collagen blocks, oxygen concentration barely affected the proportion of cells in the G0/G1 phase. Moreover, in the 3D culture, the oxygen gradient prompted cells to migrate to the edge of the collagen blocks. In brief, the developed 3D glioma tumor model can be used to explore the effect of oxygen concentration on the growth of glioma cells in vitro. This model provides a basis for future drug development for glioma diseases and the construction of an appropriate tumor model in vitro.

Supplementary Information The online version contains supplementary material available at https://doi.org/10.1007/s42242-024-00271-9.

Acknowledgements This work was supported by the National Natural Science Foundation of China (No. 52275291), the Fundamental Research Funds for the Central Universities, and the Program for Innovation Team of Shaanxi Province, China (No. 2023-CX-TD-17).

Author contributions Conceptualization: SW, SQY, LW, and XGM; methodology: SW, SQY, and NP; validation: SQY, LGB, and XYX; formal analysis: SW, SQY, XYX, and ZYH; investigation: SW, NP, and XGM; resources: DCL, XGM, and LW; data curation: SW, JKH, and LW; writing—original draft preparation: SW, SQY, NP, and LW; writing—review and editing: SW, JMO, XGM, and LW; visualization: NP and LGB; supervision: LW, DCL, and JKH; project administration: LW.

Declarations

Conflict of interest This paper is to be included in a special issue for which JMO is a guest editor. JKH is an associate editor and JMO is an editorial board member for *Bio-Design and Manufacturing*, and both were not involved in the editorial review or the decision to publish this article. The authors declare that they have no conflict of interest.

Ethical approval This research has been approved by the Animal Management Committee of Xi'an Jiaotong University (No. XJTUAE2024-1811).

References

1. Gilbert MR, Wang MH, Aldape KD et al (2013) Dose-dense temozolomide for newly diagnosed glioblastoma: a randomized phase III clinical trial. J Clinic Oncol 31(32):4085–4091. https://doi.org/10.1200/JCO.2013.49.6968
2. Wang MH, Dignam JJ, Won M et al (2015) Variation over time and interdependence between disease progression and death among patients with glioblastoma on RTOG 0525. Neuro-Oncology 17(7):999–1006. https://doi.org/10.1093/neuonc/nov009
3. Musah-Eroje A, Watson S (2019) Adaptive changes of glioblastoma cells following exposure to hypoxic (1% oxygen) tumour microenvironment. Int J Mol Sci 20(9):2091. https://doi.org/10.3390/ijms20092091
4. Hubert CG, Rivera M, Spangler LC et al (2016) A three-dimensional organoid culture system derived from human glioblastomas recapitulates the hypoxic gradients and cancer stem cell heterogeneity of tumors found in vivo. Cancer Res 76(8):2465–2477. https://doi.org/10.1158/0008-5472.CAN-15-2402
5. Wang C, Tong XM, Yang F (2014) Bioengineered 3D brain tumor model to elucidate the effects of matrix stiffness on glioblastoma cell behavior using PEG-based hydrogels. Mol Pharm 11(7):2115–2125. https://doi.org/10.1021/mp5000828
6. Florczyk SJ, Wang K, Jana S et al (2013) Porous chitosan-hyaluronic acid scaffolds as a mimic of glioblastoma microenvironment ECM. Biomaterials 34(38):10143–10150. https://doi.org/10.1016/j.biomaterials.2013.09.034
7. Kimlin LC, Casagrande G, Virador VM (2013) In vitro three-dimensional (3D) models in cancer research: an update. Mol Carcinog 52(3):167–182. https://doi.org/10.1002/mc.21844
8. Hutmacher DW, Loessner D, Rizzi S et al (2010) Can tissue engineering concepts advance tumor biology research? Trends Biotechnol 28(3):125–133. https://doi.org/10.1016/j.tibtech.2009.12.001
9. Das V, Bruzzese F, Konečný P et al (2015) Pathophysiologically relevant in vitro tumor models for drug screening. Drug Discov Today 20(7):848–855. https://doi.org/10.1016/j.drudis.2015.04.004
10. Cha J, Kim P (2017) Biomimetic strategies for the glioblastoma microenvironment. Front Mater 4:45. https://doi.org/10.3389/fmats.2017.00045
11. Musah-Eroje A, Watson S (2019) A novel 3D in vitro model of glioblastoma reveals resistance to temozolomide which was potentiated by hypoxia. J Neurooncol 142(2):231–240. https://doi.org/10.1007/s11060-019-03107-0
12. Fong ELS, Lamhamedi-Cherradi SE, Burdett E et al (2013) Modeling Ewing sarcoma tumors in vitro with 3D scaffolds. Proc Natl Acad Sci USA 110(16):6500–6505. https://doi.org/10.1073/pnas.1221403110
13. Li M, Song X, Jin S et al (2021) 3D tumor model biofabrication. Bio-Des Manuf 4(3):526–540. https://doi.org/10.1007/s42242-021-00134-7
14. Thakor J, Ahadian S, Niakan A et al (2020) Engineered hydrogels for brain tumor culture and therapy. Bio-Des Manuf 3(3):203–226. https://doi.org/10.1007/s42242-020-00084-6
15. Gomez-Roman N, Stevenson K, Gilmour L et al (2017) A novel 3D human glioblastoma cell culture system for modeling drug and radiation responses. Neuro-Oncology 19(2):229–241. https://doi.org/10.1093/neuonc/now164
16. Lv DL, Yu SC, Ping YF et al (2016) A three-dimensional collagen scaffold cell culture system for screening anti-glioma therapeutics. Oncotarget 7(35):56904–56914. https://doi.org/10.18632/oncotarget.10885
17. Huijbers IJ, Iravani M, Popov S et al (2010) A role for fibrillar collagen deposition and the collagen internalization receptor Endo180 in glioma invasion. PLoS ONE 5(3):e9808. https://doi.org/10.1371/journal.pone.0009808
18. Leitinger B (2011) Transmembrane collagen receptors. Annu Rev Cell Dev Biol 27(1):265–290. https://doi.org/10.1146/annurev-cellbio-092910-154013
19. Gilkes DM, Semenza GL, Wirtz D (2014) Hypoxia and the extracellular matrix: drivers of tumour metastasis. Nat Rev Cancer 14(6):430–439. https://doi.org/10.1038/nrc3726
20. Ma L, Li YT, Wu YT et al (2020) 3D bioprinted hyaluronic acid-based cell-laden scaffold for brain microenvironment simulation. Bio-Des Manuf 3(3):164–174. https://doi.org/10.1007/s42242-020-00076-6
21. Jiguet CJ, Baeza-Kallee N, Denicolaï E et al (2014) Ex vivo cultures of glioblastoma in three-dimensional hydrogel maintain the original tumor growth behavior and are suitable for preclinical drug and radiation sensitivity screening. Exp Cell Res 321(2):99–108. https://doi.org/10.1016/j.yexcr.2013.12.010
22. Thakor FK, Wan KW, Welsby PJ et al (2017) Pharmacological effects of asiatic acid in glioblastoma cells under hypoxia. Mol Cell Biochem 430(1–2):179–190. https://doi.org/10.1007/s11010-017-2965-5
23. Ahmed EM, Bandopadhyay G, Coyle B et al (2018) A HIF-independent, CD133-mediated mechanism of cisplatin resistance in glioblastoma cells. Cell Oncol 41(3):319–328. https://doi.org/10.1007/s13402-018-0374-8
24. Song Y, Zheng SH, Wang JZ et al (2017) Hypoxia-induced PLOD2 promotes proliferation, migration and invasion via PI3K/Akt signaling in glioma. Oncotarget 8(26):41947–41962. https://doi.org/10.18632/oncotarget.16710
25. Unwith S, Zhao HL, Hennah L et al (2015) The potential role of HIF on tumour progression and dissemination. Int J Cancer 136(11):2491–2503. https://doi.org/10.1002/ijc.28889
26. Liverani C, De Vita A, Minardi S et al (2019) A biomimetic 3D model of hypoxia-driven cancer progression. Sci Rep 9:12263. https://doi.org/10.1038/s41598-019-48701-4
27. Fang A, Hao ZY, Wang L et al (2019) In vitro model of the glial scar. Int J Bioprint 5(2):90–98. https://doi.org/10.18063/ijb.v5i2.235
28. Fang A, Li DC, Hao ZY et al (2019) Effects of astrocyte on neuronal outgrowth in a layered 3D structure. BioMed Eng OnLine 18(1):74. https://doi.org/10.1186/s12938-019-0694-6
29. Bai LG, Hao ZY, Wang S et al (2023) Biomimetic three-dimensional glioma model printed in vitro for the studies of glioma cells and neurons interactions. Int J Bioprint 9(4):1–14. https://doi.org/10.18063/ijb.715
30. Dai XL, Ma C, Lan Q et al (2016) 3D bioprinted glioma stem cells for brain tumor model and applications of drug susceptibility. Biofabrication 8(4):045005. https://doi.org/10.1088/1758-5090/8/4/045005
31. Li PC, Zhou C, Xu LS et al (2013) Hypoxia enhances stemness of cancer stem cells in glioblastoma: an in vitro study. Int J Med Sci 10(4):399–407. https://doi.org/10.7150/ijms.5407
32. Richards R, Jenkinson MD, Haylock BJ et al (2016) Cell cycle progression in glioblastoma cells is unaffected by pathophysiological levels of hypoxia. PeerJ 3:e1755. https://doi.org/10.7717/peerj.1755
33. Longati P, Jia XH, Eimer J et al (2013) 3D pancreatic carcinoma spheroids induce a matrix-rich, chemoresistant phenotype offering a better model for drug testing. BMC Cancer 13(1):95. https://doi.org/10.1186/1471-2407-13-95
34. Lo Dico A, Martelli C, Diceglie C et al (2018) Ottobrini, hypoxia-inducible factor-1α activity as a switch for glioblastoma responsiveness to temozolomide. Front Oncol 8:249. https://doi.org/10.3389/fonc.2018.00249

35. Wang P, Lan C, Xiong SL et al (2017) HIF1α regulates single differentiated glioma cell dedifferentiation to stem-like cell phenotypes with high tumorigenic potential under hypoxia. Oncotarget 8(17):28074–28092. https://doi.org/10.18632/oncotarget.15888
36. Kawai Y, Kishimoto Y, Suzuki R et al (2016) Distribution and characteristics of slow-cycling cells in rat vocal folds. Laryngoscope 126(4):E164–E170. https://doi.org/10.1002/lary.25558
37. Taniguchi M, Yamamoto N, Nakagawa T et al (2012) Identification of tympanic border cells as slow-cycling cells in the cochlea. PLoS ONE 7(10):e48544. https://doi.org/10.1371/journal.pone.0048544
38. Stummer W, Pichlmeier U, Meinel T et al (2006) Fluorescence-guided surgery with 5-aminolevulinic acid for resection of malignant glioma: a randomised controlled multicentre phase III trial. Lancet Oncol 7(5):392–401. https://doi.org/10.1016/S1470-2045(06)70665-9
39. Sarkar S, Yong VW (2009) Inflammatory cytokine modulation of matrix metalloproteinase expression and invasiveness of glioma cells in a 3-dimensional collagen matrix. J Neurooncol 91(2):157–164. https://doi.org/10.1007/s11060-008-9695-1
40. Monteiro AR, Hill R, Pilkington GJ (2017) The role of hypoxia in glioblastoma invasion. Cells 6(4):45. https://doi.org/10.3390/cells6040045
41. Rape A, Ananthanarayanan B, Kumar S (2014) Engineering strategies to mimic the glioblastoma microenvironment. Adv Drug Deliv Rev 79–80:172–183. https://doi.org/10.1016/j.addr.2014.08.012
42. Gritsenko GP, Ilina O, Friedl P (2012) Interstitial guidance of cancer invasion. J Pathol 226(2):185–199. https://doi.org/10.1002/path.3031
43. Friedl P, Alexander S (2011) Cancer invasion and the microenvironment: plasticity and reciprocity. Cell 147(5):992–1009. https://doi.org/10.1016/j.cell.2011.11.016
44. Baker BM, Chen CS (2012) Deconstructing the third dimension – how 3D culture microenvironments alter cellular cues. J Cell Sci 125(13):3015–3024. https://doi.org/10.1242/jcs.079509
45. Bellail AC, Hunter SB, Brat DJ et al (2004) Microregional extracellular matrix heterogeneity in brain modulates glioma cell invasion. Int J Biochem Cell Biol 36(6):1046–1069. https://doi.org/10.1016/j.biocel.2004.01.013
46. Wiranowska M, Ladd S, Moscinski LC et al (2010) Modulation of hyaluronan production by CD44 positive glioma cells. Int J Cancer 127(3):532–542. https://doi.org/10.1002/ijc.25085
47. Watters JJ, Schartner JM, Badie B (2005) Microglia function in brain tumors. J Neurosci Res 81(3):447–455. https://doi.org/10.1002/jnr.20485
48. Hu B, Emdad L, Kegelman TP et al (2017) Astrocyte elevated gene-1 regulates β-catenin signaling to maintain glioma stem-like stemness and self-renewal. Mol Cancer Res 15(2):225–233. https://doi.org/10.1158/1541-7786.MCR-16-0239
49. Galarneau H, Villeneuve J, Gowing G et al (2007) Increased glioma growth in mice depleted of macrophages. Cancer Res 67(18):8874–8881. https://doi.org/10.1158/0008-5472.CAN-07-0177